

Research Article

Submicron Surface Vibration Profiling Using Doppler Self-Mixing Techniques

Tânia Pereira,¹ Mariana Sequeira,¹ Pedro Vaz,¹ Ana Tomé,¹ Helena C. Pereira,^{1,2}
Carlos Correia,¹ and João Cardoso¹

¹ Instrumentation Centre, Physics Department, University of Coimbra, Rua Larga, 3004-516 Coimbra, Portugal

² Instituto Pedro Nunes, Rua Pedro Nunes-Edifício D, 3030-199 Coimbra, Portugal

Correspondence should be addressed to Tânia Pereira; taniapereira@lei.fis.uc.pt

Received 23 April 2014; Revised 9 July 2014; Accepted 10 July 2014; Published 23 July 2014

Academic Editor: Chi-Wai Chow

Copyright © 2014 Tânia Pereira et al. This is an open access article distributed under the Creative Commons Attribution License, which permits unrestricted use, distribution, and reproduction in any medium, provided the original work is properly cited.

Doppler self-mixing laser probing techniques are often used for vibration measurement with very high accuracy. A novel optoelectronic probe solution is proposed, based on off-the-shelf components, with a direct reflection optical scheme for contactless characterization of the target's movement. This probe was tested with two test bench apparatus that enhance its precision performance, with a linear actuator at low frequency (35 μm , 5–60 Hz), and its dynamics, with disc shaped transducers for small amplitude and high frequency (0.6 μm , 100–2500 Hz). The results, obtained from well-established signal processing methods for self-mixing Doppler signals, allowed the evaluation of vibration velocity and amplitudes with an average error of less than 10%. The impedance spectrum of piezoelectric (PZ) disc target revealed a maximum of impedance (around 1 kHz) for minimal Doppler shift. A bidimensional scan over the PZ disc surface allowed the categorization of the vibration mode (0,1) and explained its deflection directions. The feasibility of a laser vibrometer based on self-mixing principles and supported by tailored electronics able to accurately measure submicron displacements was, thus, successfully demonstrated.

1. Introduction

Laser Doppler velocimetry is a well-known measurement technique, widely used for accurate and remote measurement of fluid velocity and objects' displacement, velocity, and acceleration. The use of a laser diode (LD), both as an emitter and as a receiver of coherent light, allows for the capability to measure the velocity and displacement of a moving target surface. These optoelectronic elements, LDs, have been widely used in many different areas due to these remarkable features such as high sensitivity and accuracy, contactless operation, and a simplified optical scheme, when compared with most of the alternative sensors [1–4].

In order to measure the Doppler signal produced by a vibrating moving target, an optical probe based on a LD with self-mixing interference capabilities was used. This probe was tested with two different test benches in order to determine its ability to accurately measure velocity and other movement characteristics of a moving target. One test bench

was composed by a linear actuator (35 μm of amplitude) at low frequency (5–60 Hz), other with disc shaped transducers with small amplitude (0.6 μm) and high frequency (100–2500 Hz).

The optical solutions based on a LD with an algorithm for self-mixing signal processing represent an interesting tool to the determination of features of the movement described by PZ and for the study of vibration mode of PZ disc surface [5, 6].

The information of the self-mixing signals is mostly encoded in the frequency domain and, to extract important data, signal processing techniques such as the Doppler spectrogram and power spectral density was used [7]. These methods allow the extraction of the movement profile and the absolute displacement.

The features of movement measured from Doppler frequency shift during a motion of PZ enable the characterization of the relationship of energy conversion between electrical and mechanical domains.

The piezoelectric transducers have been extensively used in several applications [5]; however, there is a gap in a global characterization study of dynamic behaviour like the vibration modes of the structure, impedance spectrum, resonant frequencies, and energy balance analysis.

This study represents a global analysis of piezoelectric actuators in dynamic stage with a simple and low-cost probe for Doppler velocity measurements, which allows the determination of the vibration modes of a piezoelectric disc membrane, and the algorithms for self-mixing signal processing that allows the determination of vibration features, such as velocity and amplitude, a frequency spectrum of the PZ and energy balance analysis.

2. Material and Methods

The optical probe based on self-mixing technique was tested in two different test setups, where two types of displacement transducers were used. On a precision test setup, a piezoelectric actuator (ACT) was used, electronically driven (700 μm Physik Instrument GmbH, P-287), and biased by a high voltage linear amplifier (HVLA) Physik Instrument GmbH, E-508. This test allowed a profile error evaluation by comparing the original values defined in the system with the measurements obtained by the self-mixing signals.

A second test bench, built to characterize the dynamics of the movement, was based on a disc shaped piezoelectric element driven by an oscillating electronic circuit.

2.1. Self-Mixing Theory. The basic theory of the self-mixing effect is explained by the presence of two Fabry-Perot cavities whose parameters are sensitive to variations of the external cavity length and frequency shift of the back-scattered light [8–10]. The light from the LD is focused on the remote target and undergoes a Doppler frequency shift proportional to the target surface orthogonal velocity. A fraction of the backscattered shifted light returns to the LD cavity and coherently interferes with the original light in the laser cavity [11, 12], producing a modulated signal.

The theoretical relationship for the Doppler frequency f_d is given by (1), where v is the vector magnitude of the target's velocity, θ is the angle between the optical axis of the sensor and the velocity vector, and λ is the coherent light source [4]. Consider

$$f_d = \frac{2v \cos \theta}{\lambda}. \quad (1)$$

The interference of these two light sources (the reference beam with the original frequency and the Doppler shifted beam) produces a beat frequency related to the first order Doppler shift of the beam reflected by the moving surface [13].

For small amplitude moving targets, or limited velocity objects, this beat frequency corresponds to a much lower frequency (around MHz) than the laser light (THz) and can, therefore, be detected with a fast photodetector. In the specific case of the self-mixing LD, the photosensitive part is coupled to the laser cavity itself.

The readout LD signal is converted in a Doppler spectrogram, using a short-time Fourier transform (STFT), resulting

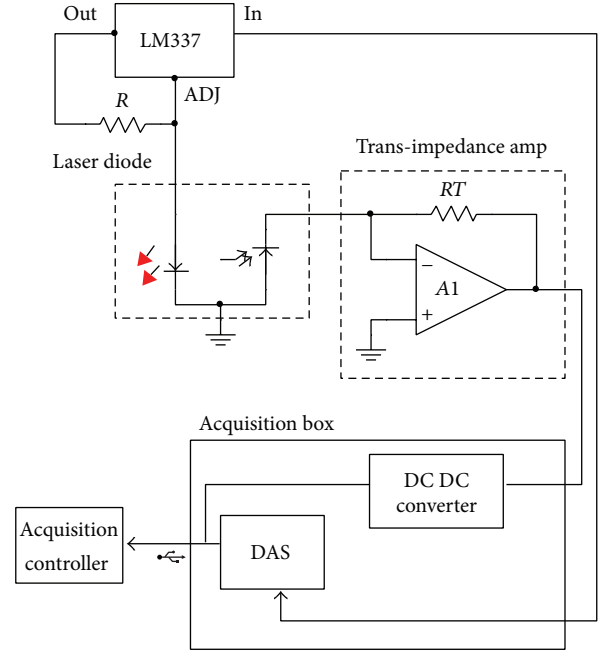


FIGURE 1: Schematic overview of the optical system.

in a frequency shift dependent plot as a function of time. The STFT assumes that the signal is stationary during the analysis interval [7, 14] and the overall spectrogram represents a sequence of spectral power distributions in a time versus frequency space.

In specific cases, such as a not constant target velocity, the statistical distribution of the measured Doppler shifts is proportional to the power spectral density (PSD) of the target velocity. The maximum Doppler frequency corresponds to the maximum velocity of the target. The peak of PSD corresponds to the dominant frequency and can be related with the velocity by (1) [6, 15].

The Doppler spectrogram allows the determination of other features of the target movement such as amplitude and period and can be used to reconstruct the movement equations that describes the target vibrations [14].

2.2. Technology. The probe makes use of a laser diode (Laser Components, ADL-65075TL Visible Laser Diode), with a peak wavelength of 635 nm and an output power of 5 mW. This LD is extensively used in optical drivers, and all the system is based on simple electronic components with an optical scheme of a single optical axis [7].

The optical probe, placed orthogonally to a printed circuit board layer and the LD, was driven by a constant current source. Figure 1 illustrates the electronics used for both driving the LD and to perform the signal readout. A constant current is imposed by a voltage regulator (LM337) in a configuration where a resistor (R) sets the output current through the load. The electronic amplification circuit consists of an ultralow bias current monolithic operational amplifier (Texas Instruments, OPA129UE4) for the current-to-voltage conversion (trans-impedance amplifier) [7].

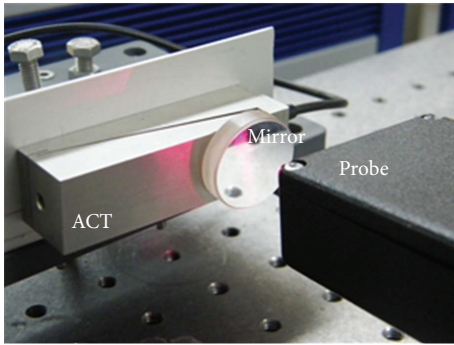


FIGURE 2: Photo of the experimental setup with ACT, mirror, and the optical probe.

The acquisition box comprises a data acquisition system (DAS), a DC/DC converter, and an USB connection for primary power supply and interface with the host controller. The DC/DC circuit converts the standard USB +5 V to the voltages required by the analog electronics (± 15 V) of the optical probe [7].

The signals were acquired using a 16-bit resolution data acquisition system (National Instruments, USB-6343) and stored for offline analysis using Mathworks MATLAB.

2.3. Test Bench I. The test bench I, which is represented in Figure 2, was based on a piezoelectric actuator (ACT) mechanically coupled to a mirror surface that acts as the moving target. For bench procedure, a sinusoidal driving signal was used, thus, providing a single frequency oscillatory movement. This test was designed to evaluate the ability of the optical probe to measure the velocity and amplitude in a micron range.

The sinusoidal movement signal was provided by an actuator (ACT in Figure 2) driven by the HVLA that amplifies to the appropriate high voltage level the Agilent 33220A output. The mirror attached to the actuator reproduced a pure sinusoidal movement with $35 \mu\text{m}$ of amplitude.

In the velocity study, several frequencies, from 5 to 60 Hz, were tested with the optical probe axis perpendicular to the mirror surface in order to detect the Doppler frequency modulation imposed to the reflected light.

2.4. Test Bench II. In a second test bench the ACT was replaced with a piezoelectric disc and finely polished to improve the reflection properties of the vibrating surface. A circularly-shaped piezoelectric sounder, MURATA 7BB-35-3, with 23 mm electrode size diameter and 2.8 ± 0.5 kHz resonant frequency, was used.

To determine the characteristics of the PZ vibration, a sinusoidal voltage signal, from an Agilent 33220A arbitrary waveform generator, was used as a driving signal for the sounder.

Figure 3 depicts this test bench apparatus with a three axis linear precision positioner (T-LA28A from ZABER Linear Actuator, 28 mm travel range with RS-232 interface) that allows precise control of the actuator position relative to the

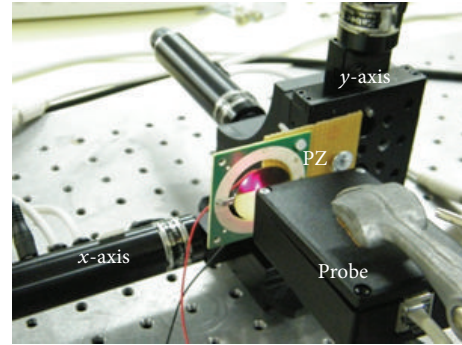


FIGURE 3: Photo of the experimental setup with PZ disc fixed in three linear actuators in front of optical probe.

probe. The PZ is welded at two points at the edge of the metal disc to guarantee free vibration of the piezo wafer.

3. Results and Discussion

The self-mixing signals readout from the optical probe were processed in order to characterize the mechanical dynamics of the target. Complementally, a study of the errors associated to this measure was performed.

3.1. Actuator Velocity Assessment. The self-mixing signals were sampled at 100 kHz. Figure 4 shows the power spectrum of the self-mixing signals obtained when the sinusoidal frequency that drives the ACT is swept from 5 to 60 Hz, with constant amplitude of the $35 \mu\text{m}$. The Doppler frequency is computed as the maximum peak in the power spectrum calculated for the signals (magenta dots). It is clearly visible that the Doppler frequency increases when the ACT velocity also increases. However there is a nonlinear correlation between these two variables that were expected to be linearly correlated. This behaviour results from the operating limits the HVLA when it drives high capacitive loads. Regarding the inherent electrical capacitance of the actuator ($290 \text{ nF} \pm 20\%$), the response curve of the HVLA presents a decreasing amplitude for frequencies values higher than 45 Hz.

In Figure 4 it is also possible to identify another frequency component, which is twice the Doppler frequency, representing a second harmonic generated by the multiple reflections at the dielectric mirror used in the test setup. An interface between two different dielectric media is a source of second and third-harmonic components which are clearly visible in the spectrogram (Figure 4) [16]. In the power spectrum plot the presence of a strong component at 28.52 kHz and at 42.97 kHz is also clear, for all the analysed signals. This effect results from an interference in the data acquisition system (DAS), which is easily proved since the two peaks remain in the spectrum even for acquisitions with the probe turned off. However, these interference peaks do not affect our conclusions on the target's dynamics, if properly considered during processing.

The theoretical relationship for the Doppler frequency (1) allows the determination of the ACT velocity. To solve the equation that describes the sinusoidal movement, the

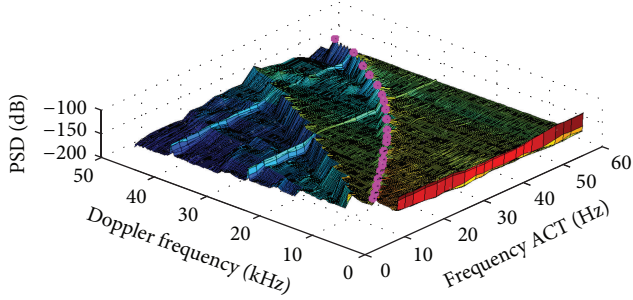


FIGURE 4: PSD generated by the self-mixing signals for a sinusoidal vibration of the ACT (movement frequencies between 5 to 60 Hz). The power spectral characteristics evidence the behaviour of Doppler frequency with the ACT frequency marked with magenta dots.

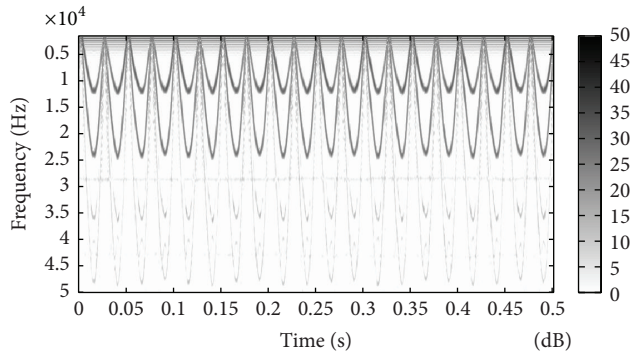


FIGURE 5: Spectrogram for a self-mixing signal at a 20 Hz vibration of the actuator ACT. Conventional gray scale representing the top 50 dB of the signal.

amplitude of the ACT displacement needs to be assessed. The spectrogram is considered to be the most valuable tool to derive the target movement from the self-mixing signals. This time dependent spectral description of the signal is obtained through a sequence of STFTs over the analysis interval, providing a two-dimensional matrix with the coefficients proportional to the frequencies present in each time window (Figure 5). In this grey scale plot the predominant frequencies are represented by the darker colours (50 dB). The successively attenuated harmonics are clearly visible as lighter traces on the STFT plot.

The sinusoidal movement is described by (2), where A is the amplitude of the movement and w is the angular frequency:

$$\begin{aligned} x(t) &= A \sin(wt), \\ v(t) &= Aw \cos(wt), \\ a(t) &= -Aw^2 \sin(wt). \end{aligned} \quad (2)$$

These expressions are related to (1) leading to the equation that describes the velocity $v = Aw$.

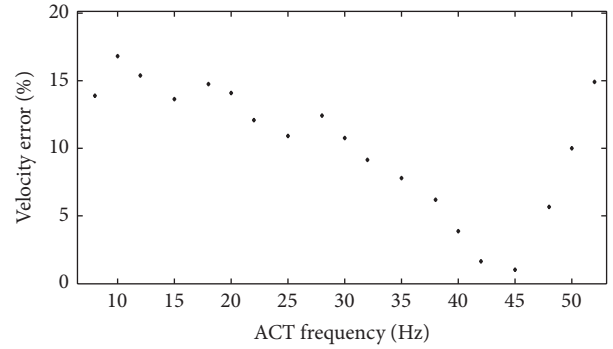


FIGURE 6: Error evolution for the velocity determined in the different frequencies tested.

3.2. Evaluation Error in Actuator Movement. The velocity computation, according to the previously described expressions, revealed a particular distribution illustrated by Figure 6. The comparison between these values obtained from the self-mixing signal analysis and the real values imposed on the actuator shows an average error of 10% for the amplitude and velocity values.

This error is inversely proportional to the ACT driving frequency for values below 45 Hz and quickly increases above this value. This behaviour is explained by the performance degradation of the actuator for this frequency range, as mentioned earlier.

The relative error is higher at lower velocities and decreases when the velocity increases. Similar results obtained by other authors [4, 17–19] support our observations. It is shown that the method is not sensitive to slow movements, that is, low frequencies, since the Doppler frequency is too close to the fundamental frequency and consequently cannot be clearly distinguished.

The movement amplitude is estimated from two variables extracted from the self-mixing analysis: v and w . The amplitude mean value obtained is $33.8 \mu\text{m}$ with standard error of $5.6 \mu\text{m}$. The error associated to these values produces an amplitude error of less than 20% in all measurements.

3.3. PZ Velocity Measurements. Higher Doppler frequencies are expected for the test bench II that was used to characterize the piezoelectric transducer. As the sampling frequency must always be higher than twice the measured beat frequency (from the Nyquist-Shannon theorem), the self-mixing signals were sampled at the higher possible frequency supported by the DAS, that is, 500 kHz.

To study the PZ vibration it was necessary to select the best surface region on the PZ to acquire the signals. In order to build the PZ vibration profile, a systematic disc surface scan was performed. The axis linear precision positioners were used in 28 incremental steps, both in x -axis and in y -axis, resulting in a square image (28×28 pixel). The signals were acquired for a fixed vibration frequency of 600 Hz far enough from the PZ resonance frequency expected to be around 2.8 ± 0.5 kHz. The Doppler shifted frequencies determined are represented by a colour scheme in Figure 7. From the

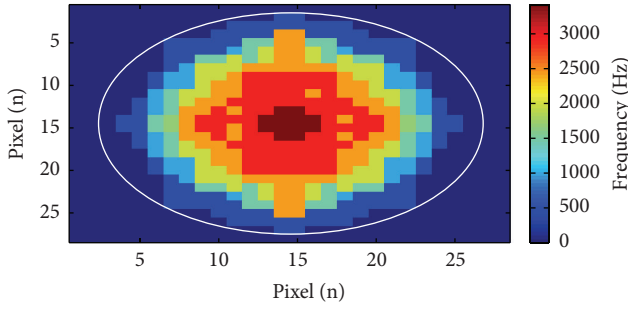


FIGURE 7: The mode shape (0, 1) of the PZ disc vibration obtained by the Doppler frequencies. The scales represent the number of pixels, and the colour code represents the Doppler frequency (in Hz) for each pixel.

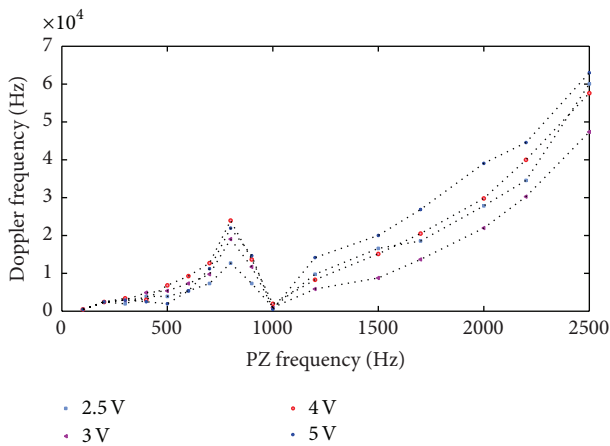


FIGURE 8: Typical curve response for the Doppler frequency obtained from the several acquisitions with different amplitudes (2.5 V, 3 V, 4 V, and 5 V) of the self-mixing signals for different frequencies in the PZ movement.

observation of this image it can be concluded that points near the disc fixation site (left and right peripheral points) present low vibration, that is, the determined Doppler frequency is close to zero. This vibration absence, corresponds to a null velocity, and account for the elliptical shape of the vibration area.

The vibration amplitude, in the centre of disc, was estimated to be $0.6 \mu\text{m}$ by using the central Doppler information presented in the PZ disc scanning.

Figure 7, obtained from the surface scan, can be used to identify the vibration mode of the PZ disc and explain the deflection directions on the disc. The vibration mode (0, 1) acts like a monopole source and represents the most efficient mode concerning the transfer of vibrational energy [5].

The frequency spectrum of the PZ measured by the optical probe is shown in Figure 8. The PZ disc transducer was swept by frequencies from 100 to 2500 Hz, and, for each scan, four slightly different amplitudes were tested. Frequencies above 2.5 kHz were tested but the power spectrum of the self-mixing becomes very complex, making the Doppler frequency determination very hard most likely due to the resonance effect expected for these frequencies.

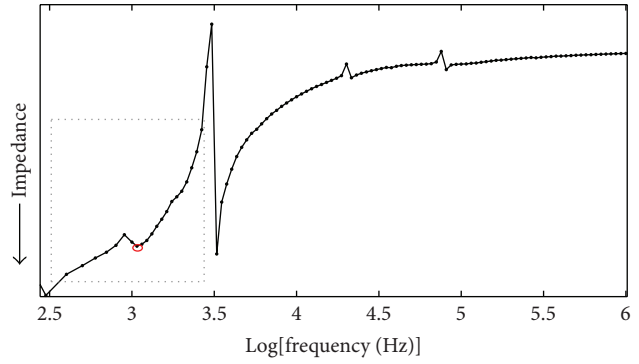


FIGURE 9: Impedance profile of a piezoelectric disc. The frequencies are represented in logarithmic scale. Dashed box define the frequency window that corresponds to the frequencies analyzed for the PZ response; red dot makes a second antiresonance point in 1 kHz.

The behaviour of the Doppler frequency curve (Figure 8) shows an inflection point when the PZ vibrates at 1 kHz that can be properly understood considering the impedance analysis of the PZ (Section 3.4).

In the test bench the piezoelectric layer converts electrical energy into mechanical energy. When excited at the resonant frequency, the PZ will resonate freely with higher amplitude than at any other frequencies. In the vicinity of this resonant frequency, an anti-resonant frequency is expected, with a consequent impedance maximum and, therefore, minimum oscillation amplitude.

The ability to transform electrical energy into mechanical energy depends on the frequency response of the PZ and can be measured through the impedance spectrum.

3.4. PZ Impedance Measurements. An electrical impedance spectroscopy (EIS) system [20] was used to obtain the spectrum of impedance profile (Figure 9), and a comparative analysis was performed with profile estimated from the optical signals.

The resonant frequency, that is, minimum of impedance, occurs at 3 kHz which corresponds to the value expected for the PZ used in this study. The antiresonant frequency, that is, maximum impedance, occurs immediately afterwards, at about 3.3 kHz. For the antiresonant frequency, the PZ disc shows almost no displacement and no reproductive behaviour to the applied voltage, showing minimum conversion of electrical energy into mechanical energy. There is another maximum in the impedance curve that explains the particular behaviour for the determined Doppler frequencies. At around 1 kHz (red dot mark in Figure 9) the Doppler frequency is close to zero due to the higher impedance of PZ. The dashed box in Figure 9 defines the frequency window that is represented in Figure 8 and exhibits the same wave profile, which explains the behaviour of PZ vibration and Doppler frequencies obtained.

3.5. PZ Energy Study. The electric to mechanical energy conversion in the actuator accounts for the mechanical

movement (oscillation) of the PZ element and its adjacent materials, when the sinusoidal voltage is applied. The electric power delivered to the PZ is evaluated by measuring its electrical current using a sense resistor. The instantaneous electric power for a 600 Hz frequency was found to be 2.9×10^{-3} W.

The mechanical power was computed as the sum of the power of each pixel, as seen in Figure 7: $P = \sum m_p a_p v_p$ where a_p and v_p are acceleration and velocity, respectively, directly derived from the corresponding Doppler frequencies, and m_p is the mass of the vibrating pixel, estimated from its dimensions and from the physical properties of the disc [21]. A total mechanical power of 6.01×10^{-6} W was computed.

The efficiency of the energy conversion process, understood as the ratio between the electrical input and the mechanical output powers, was computed to be 2.07×10^{-3} . A significant part of the electric energy seems to be lost due to the source-load impedance mismatch at 600 Hz, which is very far from equality, the condition for maximum power transfer. The low conversion efficiency of piezoelectric materials also contributes to these final results that are similar to others [21, 22].

4. Conclusions

A low-cost optical system able to acquire a self-mixing signal from a vibration target has been assembled and was used to develop an algorithm for estimation of the movement features. The new optical system is portable, compact, lightweight and it was designed with low power and off-the-shelf materials, easy to assemble and align, in order to be considered as an interesting solution.

The developed algorithm uses well established methods for signal processing of self-mixing Doppler signals, such as the STFT and PSD for the determination of the features of the movement. This method allows the estimation of the movement equations and the evaluation of velocity and amplitude with an average error of less than 10%.

A test bench apparatus based on electromechanical actuator evidences limitations on its operation limits due to the electronic circuitry that introduces an error for movements with frequencies upper than 45 Hz.

The results obtained by the Doppler signals enabled the construction of the vibration curve of the PZ, and it was confirmed by the impedance spectroscopy analysis.

The scan of all regions of the PZ disc allowed the identification its main vibration mode (0, 1) and explained the deflection directions in the disc.

The energy balance analysis allowed the evaluation of the electromechanical characteristics of the piezoelectric disc, under dynamic conditions, and the determination of the efficiency of electrical power conversion into mechanical power.

Finally, it has been demonstrated that a laser vibrometer based on the self-mixing effect, with a simple optical apparatus, can accurately perform measurements of velocity and displacements in sub-micron vibrations amplitudes.

Conflict of Interests

The authors declare that there is no conflict of interests regarding the publication of this paper.

Acknowledgments

The authors acknowledge the support from Fundação para a Ciência e Tecnologia (FCT) for funding (SFRH/BD/79334/2011). Project developed under the initiative of QREN funding by UE/FEDER, through COMPETE—Programa Operacional Factores de Competitividade.

References

- [1] C. Bes, G. Plantier, T. Bosch, and S. Member, "Displacement measurements using a self-mixing laser diode under moderate feedback," *IEEE Transactions on Instrumentation and Measurement*, vol. 55, no. 4, pp. 1101–1105, 2006.
- [2] A. Magnani, M. Norgia, and A. Pesatori, "Optical displacement sensor based on novel self-mixing reconstruction method," in *Proceedings of the 9th IEEE Sensors Conference (SENSORS '10)*, pp. 517–520, Kona, Hawaii, USA, November 2010.
- [3] M. Norgia and A. Pesatori, "New low cost analog self-mixing vibrometer," in *Proceedings of the 9th IEEE Sensors Conference*, pp. 477–480, November 2010.
- [4] Z. Yuyan, W. Yu tian, and R. Rui, "Laser Doppler Velocimetry based on self-mixing effect in vertical-cavity surface-emitting lasers," in *Proceedings of the 8th International Conference on Electronic Measurement and Instruments, Principle of Self-Mixing Type 3 Experimental Description*, pp. 1-413–1-416, 2007.
- [5] M. Olfatnia, V. R. Singh, T. Xu, J. M. Miao, and L. S. Ong, "Analysis of the vibration modes of piezoelectric circular micro-diaphragms," *Journal of Micromechanics and Microengineering*, vol. 20, no. 8, Article ID 085013, 2010.
- [6] L. Scalise, Y. Yu, G. Giuliani, G. Plantier, and T. Bosch, "Self-mixing laser diode velocimetry: application to vibration and velocity measurement," *IEEE Transactions on Instrumentation and Measurement*, vol. 53, no. 1, pp. 223–232, 2004.
- [7] T. Pereira, P. Vaz, T. Oliveira et al., "Empirical mode decomposition for self-mixing Doppler signals of hemodynamic optical probes," *Physiological Measurement*, vol. 34, no. 3, pp. 377–390, 2013.
- [8] D. Guo and M. Wang, "New absolute distance measurement technique with a self-mixing interferometer," *Journal of Physics: Conference Series*, vol. 48, pp. 1381–1386, 2007.
- [9] J. Perchoux, H. E. Dougan, F. Bony, and A. D. Rakić, "Photodiode-free doppler velocimeter based on self-mixing effect in commercial VCSELs," in *Proceedings of the IEEE Sensors*, pp. 290–293, Lecce, Italy, October 2008.
- [10] U. Zabit, O. D. Bernal, and T. Bosch, "Self-mixing sensor for real-time measurement of harmonic and arbitrary displacements," in *Proceedings of the IEEE International Instrumentation and Measurement Technology Conference*, vol. 2, pp. 754–758, May 2012.
- [11] M. Wang, "Fourier transform method for self-mixing interference signal analysis," *Optics and Laser Technology*, vol. 33, no. 6, pp. 409–416, 2001.

- [12] Y. Zhang, M. Zheng, W. Hu, and M. Chen, "Displacement estimation based on phase unwrapping technique in optical self-mixing system," in *Proceedings of the 1st International Conference on Instrumentation and Measurement, Computer, Communication and Control (IMCCC '11)*, pp. 160–163, October 2011.
- [13] G. Giuliani, S. Bozzi-Pietra, and S. Donati, "Self-mixing laser diode vibrometer," *Measurement Science and Technology*, vol. 14, no. 1, pp. 24–32, 2003.
- [14] J. Hast, R. Myllylä, H. Sorvoja, and J. Miettinen, "Arterial pulse shape measurement using self-mixing effect in a diode laser," *Quantum Electronics*, vol. 32, no. 11, pp. 975–980, 2002.
- [15] R. Wunenburger, N. Mujica, and S. Fauve, "Experimental study of the Doppler shift generated by a vibrating scatterer," *Journal of the Acoustical Society of America*, vol. 115, no. 2, pp. 507–514, 2004.
- [16] T. Y. F. Tsang, "Optical third-harmonic generation at interfaces," *Physical Review A*, vol. 52, no. 5, pp. 4116–4125, 1995.
- [17] L. Krehut, J. Hast, E. Alarousu, and R. Myllylä, "Low cost velocity sensor based on the self-mixing effect in a laser diode," *Opto-Electronics Review*, vol. 11, no. 4, pp. 313–319, 2003.
- [18] T. Bosch, N. Servagent, and S. Donati, "Optical feedback interferometry for sensing application," *Optical Engineering*, vol. 40, no. 1, pp. 20–27, 2001.
- [19] M. Laroche, L. Kervevan, H. Gilles, S. Girard, and J. K. Sahu, "Doppler velocimetry using self-mixing effect in a short Er-Yb-doped phosphate glass fiber laser," *Applied Physics B*, vol. 80, no. 4-5, pp. 603–607, 2005.
- [20] E. Borges, M. Sequeira, A. F. V. Cortez et al., "Bioimpedance parameters as a risk factor to assess pine decay: an innovative approach to the diagnosis of plant diseases," in *Proceedings of the 6th International Conference on Bio-Inspired Systems and Signal Processing (BIOSIGNALS '13)*, Angers, France, 2013.
- [21] T. Jin, A. Takita, M. Djamal, W. Hou, H. Jia, and Y. Fujii, "A method for evaluating the electro-mechanical characteristics of piezoelectric actuators during motion," *Sensors*, vol. 12, no. 9, pp. 11559–11570, 2012.
- [22] J. Václavík and P. Mokřý, "Measurement of mechanical and electrical energy flows in the semi-active piezoelectric shunt damping system," *Journal of Intelligent Material Systems and Structures*, vol. 23, no. 5, pp. 527–533, 2012.



Hindawi

Submit your manuscripts at
<http://www.hindawi.com>

